

# Effect of Bromide on the Interfacial Structure of Aqueous Tetrabutyl-Ammonium Iodide: Photoelectron Spectroscopy and Molecular Dynamics Simulations

**Bernd Winter<sup>\*</sup>, Ramona Weber, and Ingolf V. Hertel**

*Max-Born-Institut für Nichtlineare Optik und Kurzzeitspektroskopie,*

*Max-Born-Str. 2A, D-12489 Berlin, Germany*

**Manfred Faubel**

*Max-Planck-Institut für Strömungsforschung,*

*Bunsenstr. 10, D-37073 Göttingen, Germany*

**Luboš Vrbka and Pavel Jungwirth<sup>\*</sup>**

*Institute of Organic Chemistry and Biochemistry, Academy of Sciences of the Czech Republic and  
Center for Complex Molecular Systems and Biomolecules, Flemingovo nám. 2, 16610 Prague 6,  
Czech Republic*

## Abstract

Solvation of surface-active tetrabutyl-ammonium iodide (TBAI) in pure liquid water and in sodium bromide aqueous solution was investigated by photoelectron spectroscopy and by molecular dynamics simulations. Using VUV synchrotron radiation the experimental technique is particularly suitable to investigate the solution surface. The observed anion signal intensity changes in the photoemission spectra, in the presence of bromide, are consistent with the varying propensities of the different ions for the solution interface, analyzed in terms of hydrophobic, polarization, and ion-ion interactions. While the cations are surface-bound due to hydrophobic interactions, the anions are driven to the vacuum/solution interface by their large polarizability and size. Iodide is more polarizable, and hence more surface-active than the smaller bromide, which explains the relatively small decrease of the iodide photoemission signal when TBAI is dissolved in bromide aqueous solution.

**Keywords:** tetrabutyl-ammonium, iodide, bromide, photoelectron spectroscopy, molecular dynamics, interface, aqueous solvation

---

<sup>\*</sup>To whom correspondence should be addressed.

E-mail: bwinter@mbi-berlin.de or pavel.jungwirth@uochb.cas.cz

## I. Introduction

The interactions between water molecules and dissolved ions are of crucial importance for many physical and chemical processes in biological systems, in the atmosphere, and in technological applications. Recent experimental and theoretical studies of the interfacial structure of aqueous solutions suggest that certain hydrophilic aqueous ions are located within the solution surface,<sup>1-7</sup> which would contrast the commonly assumed thermodynamic picture of an interface depleted of ions.<sup>8,9</sup> Specifically, non-polarizable ions, such as alkali metal cations or fluoride, have been shown by molecular dynamics (MD) simulations, using polarizable force fields, to be repelled from the interface.<sup>5</sup> Contrarily, soft, polarizable simple ions, such as the heavier halides  $\text{Cl}^-$ ,  $\text{Br}^-$ , and  $\text{I}^-$ , exhibit surface affinity, the effect scaling with the anion polarizability and size.<sup>4,5,7</sup> This mechanism is different from the hydrophobic interactions for ionic surfactants, containing for instance aliphatic chains, that also leads to the accumulation at the aqueous surface.<sup>10-12</sup>

This study focuses on the effect of the counter-anions, iodide vs bromide, on the surface behavior of tetrabutyl-ammonium (TBA) which is a prototype of an ionic surfactant. TBA is in fact one of the most efficient and intensively investigated phase-transfer catalysts.<sup>13</sup> In a previous work it was shown how the iodide propensity for the surface is affected by the counter-cation.<sup>11,14</sup> When  $\text{Na}^+$ , which is not surface-active, is the counter-ion iodide tends to be moved toward the bulk due to Coulomb attraction.<sup>14</sup> In contrast, when an ionic surfactant, such as  $\text{TBA}^+$ , is the counter-ion iodide is rather dragged to the solution interface.<sup>11</sup> In the present work we contrast both photoemission spectra and MD simulations for TBAI dissolved in pure water vs aqueous bromide solution. An important question is whether or not the addition of bromide counter-ions, in excess compared to the iodide concentration, influences the surface behavior of a strong surfactant such as  $\text{TBA}^+$ . Is there for instance a noticeable competition for surface sites of the different anions, and how would that affect the surface structure in terms of anion vs cation distribution at the interface, or with respect to the number density of the completed surface monolayer?

## II. Experimental and Computational Details

### A. Experimental

Photoelectron spectroscopy is combined with the liquid microjet technique. The 6  $\mu\text{m}$

diameter liquid microjet is generated in a high-vacuum environment yielding nearly collisionless evaporation.<sup>15</sup> Briefly, the jet, having a temperature of 4° C, is formed by injecting the liquid at 80 bar He pressure through a 10 µm diameter orifice.<sup>15,16</sup> At the exit of the nozzle the beam contracts to 6 µm acquiring a final velocity of about 125 ms<sup>-1</sup>.<sup>15,17</sup> For 3-5 mm downstream from the nozzle the beam is laminar having a smooth surface. The working pressure is 10<sup>-5</sup> mbar. Photoelectrons pass through a 100 µm orifice, which separates the jet main chamber from the electron detection chamber (10<sup>-9</sup> mbar) housing a hemispherical electron energy analyzer equipped with a single electron multiplier detector. Highly demineralized water was used, and salts were of highest quality commercially available (p.a., Aldrich). Concentrations throughout the paper are given in molality (1m = 1 molal).

The photoemission measurements were performed at the MBI undulator beamline (U125) at the synchrotron radiation facility BESSY, Berlin. This beamline delivered photon energies up to 180 eV, at >6000 energy resolution. For the present experiments the resolution was reduced though, in favor of the photoemission signal to about 100 meV, since the intrinsic widths of the liquid features are typically >0.5 eV. At a photon flux of about 4·10<sup>12</sup>/s per 0.1 Å ring current, count rates on the order of 10-100 counts per second at peak maximum were obtained. The synchrotron light intersects the laminar liquid jet at normal incidence, and electron detection is normal to both the jet direction and the light polarization vector.

## Computational

Construction of the simulation cells proceeded similarly as in our previous studies.<sup>11,12</sup> A box containing 863 POL3 water molecules<sup>18</sup> (approximate dimensions 31×31×30 Å<sup>3</sup>) was elongated in the z-direction to 100 Å. Periodic boundary conditions were applied in all three dimensions to produce an infinite water slab in the xy-plane with two air/water interfaces perpendicular to the z-axis. 1 or 16 TBAI ion pairs together with 16 NaBr ion pairs were added to the simulation cell. Initially, 8 NaBr pairs were placed at each interface. For the more concentrated system, 8 TBAI ion pairs were initially placed on each side of the water slab as well, while for the more dilute system a single TBAI ion pair was placed on one of the slab surfaces.

Classical equations of motion were integrated numerically with a time step of 1 fs. Van der Waals and electrostatic interactions were cut off at 12 Å. A smooth particle mesh Ewald procedure<sup>19</sup>

was used for accounting for the long range electrostatic interactions. All bonds involving hydrogen atoms were frozen using the SHAKE algorithm.<sup>20</sup> Temperature was held fixed (except for the initial heating period) at 300 K. All the simulations were performed in the canonical ensemble (NVT).

Simulation protocol started with 15000 steps of steepest descent minimization to eliminate potential bad contacts. MD simulations were started with velocity assignment corresponding to 10 K. During a 50 ps of heating, temperature was gradually increased to 300 K. 500 ps equilibration and 1 ns production period followed. Coordinates were saved for further analysis every 500 steps, i.e., every 0.5 ps.

MD simulations were carried out using the AMBER7 software package<sup>21</sup> employing the parm99.dat parameter set<sup>22</sup> with polarizability included in the force field.<sup>23</sup> Slightly modified anion polarizabilities were used.<sup>24</sup> A self-consistent iterative procedure was used to converge the induced dipoles.

### III. Results and Discussion

#### A. Photoemission Measurements

Figure 1 shows typical photoemission spectra of 0.02m TBAI aqueous solution (top), of 0.02m TBAI dissolved in 1m aqueous NaBr (center), and of 1m NaBr aqueous solution (bottom). The spectra were obtained for 100 eV photon energy. Electron binding energies are presented with respect to vacuum,<sup>14,16</sup> and relative intensities of the three traces are scaled to the synchrotron beam current. Lower intensities of the water photoemission signal (liquid water orbital emission  $1b_1$ ,  $3a_1$ ,  $1b_2$ ,  $2a_1$ , is labeled in the figure) in the top and center traces are attributed to the formation of the surfactant single surface layer. Notice that for 0.02m TBAI concentration the segregation monolayer is completely developed (surface coverage of  $0.9 \cdot 10^{14} \text{ cm}^{-2}$ ).<sup>11</sup> The strong signal at 53.8/55.5 eV in the 0.02m TBAI solution spectrum arises from I(4d) emission which is enhanced at the photon energy used due to a shape resonance.<sup>11,14</sup> There is another effect though. As shown recently, about the same I(4d) intensity is obtained for NaI aqueous solution, however at 80 times higher concentration, confirming TBAI surface segregation. A segregation factor of 70 was deduced from the measurements.<sup>11</sup> Notice that for the photon energy used only the first few solution layers are probed. Emission from I(5p) gives rise to the weak doublet near 7.7/8.8 eV, and in addition, an iodide Auger peak occurs near 68 eV. Peak

positions and widths have been previously analyzed in detail for various alkali halide aqueous solutions.<sup>14</sup> Signal from  $\text{TBA}^+$  is barely seen due to lower photoionization cross sections.<sup>11</sup> The only noticeable contribution is the small intensity increase in the region of the water  $1b_2$  emission. The broad signal background observed in all spectra results primarily from secondary electrons (inelastic scattering in the bulk liquid); there are though some additional weaker contributions which are analogous to optical excitations.<sup>11,14</sup>

In the 1m NaBr spectrum (bottom) features of both anions and cations can be observed:  $\text{Br}^-$  ( $3d$ ) and  $\text{Br}^-(4p)$  emission at 73.2/74.3 eV and near 8.8 eV, and  $\text{Na}^+(2p)$  emission at 68 eV. The center spectrum in Figure 1, for 0.02m TBAI in 1m NaBr mixed solution, exhibits all aforementioned peaks (occurring at identical energies), however, with different intensities relative to the top and bottom traces, respectively. The main effect on dissolving TBAI in pure water (top) as compared to dissolution in aqueous 1m NaBr solution (center) is a 60% decrease of the iodide signal for the mixed solution. At the same time slightly higher  $\text{Br}^-$ , but reduced  $\text{Na}^+$  signal can be observed for the mixed solution as compared to the 1m NaBr solution (bottom). Apparently, this results from the competition for surface sites, in close vicinity to the  $\text{TBA}^+$  cations, between iodide and bromide anions. Hence, for the mixed solution also bromide will be accommodated in the surface layer. Consequently the bromide photoemission signal is expected to rise. In view of the ca. 50 times higher bromide concentration (1m NaBr vs 0.02m TBAI) the 60% effect is in fact not large, which can be explained by the larger propensity of iodide for the solution surface (see below). Notice that the  $\text{Na}^+$  signal attenuation for the mixture (center trace) is caused by the surface segregation layer (similarly to the water signal).

## B. MD Results

Typical snapshots from simulations of a single TBAI ion pair and 16 such pairs in a slab containing a  $\sim 1$  M aqueous solution of NaBr are depicted in Figs. 2a and 2b. Already from these snapshots we qualitatively see the segregation patterns of the ions in the interfacial layer, both for a low concentration of TBAI and for its high concentration (where the surface monolayer is filled and few  $\text{TBA}^+$  cations are pushed into the aqueous bulk).

Counter-ion effects and the role of polarizability on the distribution of ions across the aqueous slab can be best deduced from the density profiles of the ions studied. To this end the simulation cell

was divided into 0.2 Å thick slices parallel to the solution/vapor interface, and the distributions of the nitrogen atoms of TBA<sup>+</sup>, Na<sup>+</sup> cations, the two counter-anions (Br<sup>-</sup> and I<sup>-</sup>), as well as the water oxygen atoms across the aqueous slab were averaged over the whole trajectory.

The resulting normalized plots are displayed for one single TBAI ion pair (Fig. 3a) and for 16 (8 per each interface) TBAI pairs (Figure 3b). For the lower concentration of TBAI two overlapping sharp peaks are obtained, corresponding to the strong surface affinity of both the TBA cation and iodide anions. Bromide also shows certain preference for the interface (maximum surface enhancement by a factor of two), but not nearly as strong as iodide (100 % in the interfacial layer), despite the fact that bromide is 16 times more concentrated than iodide. Sodium cations are repelled from the interface. The preference of TBA<sup>+</sup> cations for the interface, due to the hydrophobic interactions of the butyl chains, and likewise the propensity of iodide for the surface due to its large polarizability and the charge neutralization effect, are consistent with our recent study on aqueous TBAI solutions.<sup>11</sup>

Trends in the preference for the interface of the halides follow the Hofmeister series (I<sup>-</sup> > Br<sup>-</sup> > Cl<sup>-</sup> > F<sup>-</sup>),<sup>25</sup> and can be assigned to increasing polarizability and size of anions when going from F<sup>-</sup> to I<sup>-</sup>.<sup>6</sup> This is quantitatively observed in Fig. 3a for bromide vs iodide. The bromide interfacial peak is slightly shifted towards the bulk, when compared to iodide, however, both peaks correspond to the outermost layer.

Upon increasing the TBAI concentration to a region which, for the pure TBAI solution, corresponds to the completed segregation monolayer,<sup>11</sup> iodide anions are pushed strongly toward the interface (Fig. 3b). The iodide to bromide concentration ratio is almost twice as large at the interface than in the bulk. Broadening of the density peaks can be related to sterical confinement at this near-saturation coverage. Since ionic surfactants do not tend to form more than one layer, excess cations then move into the bulk, contributing also to the broadening of the slab by crowding out water molecules.

When the intensity of the iodide interfacial peak for the more concentrated system (Fig. 3b) is compared to our previous results for aqueous TBAI without addition of NaBr,<sup>11</sup> a 35% decrease can be observed. The experimentally observed decrease is 60%, however, that value corresponds to concentration ratio I:Br 1:50, whereas in the simulation the concentration ratio is 1:1. As a matter of

fact, for strong surfactants (such as TBA<sup>+</sup>) it is probably more meaningful to compare the degree of surface coverage rather than concentrations; in this respect the conditions of the simulation are much closer to the experiment. In any case, it can be safely deduced that the intensity decrease would be larger for concentration ratios closer to the experiment. This is, however, not feasible in our simulations, since for the experimental concentrations there would be less than a single iodide in the unit cell.

One might possibly expect that the observed shifts of the iodide and bromide maxima could result in creation of an electric double layer, however, careful analysis of the charge profiles across the whole slab does not confirm this. Charges of TBA<sup>+</sup>, I<sup>-</sup>, and Br<sup>-</sup> residing within the same surface layer effectively cancel each other, and the remaining charge (i.e., Br<sup>-</sup> in the “subsurface layer”) is compensated mainly by the preferential orientation of the water molecules<sup>11,12</sup> and by the Na<sup>+</sup> cations present near the interface. This water orientation also leads to the appearance of a weak surface electrical double layer which is, however, almost negligible, and is observed already in neat water simulations. Finally, there is another region of positive charge below this double layer corresponding to a higher population of Na<sup>+</sup> cations attracted close to the interface by the Coulombic forces.

Relative shifts of the iodide and bromide density maxima are caused by their different affinity to the interface and by steric reasons. For the higher concentration of TBAI there is not enough free space in the interfacial layer to accommodate both TBA<sup>+</sup> and counter-anions, therefore, the anion with a smaller affinity to the interface (Br<sup>-</sup>) is preferentially shifted towards the bulk (Fig. 2b).

The orientation of the hydrophobic aliphatic chains of TBA<sup>+</sup> with respect to the normal to the surface is affected by the presence of the bromide anions at the interface. As discussed in detail in our previous study,<sup>11</sup> in aqueous TBAI (without added NaBr) there is a broad peak between 75° and 150° for the single ion pair, while two orientational peaks around 90° and 150° arise for the concentrated system. When NaBr is added, angles around 70° and 170° are preferred for the single TBAI ion pair, i.e. butyl chains either lie on the surface or point toward the inside of the slab. For the more concentrated system, angles around 10° - 40° and 170° are preferred. The more profound preference for orientations perpendicular to the surface is due to the higher particle density at the interface requiring butyl chains to be oriented towards the gas phase, requiring thus less space.

Enrichment of Br<sup>-</sup> and I<sup>-</sup> at the interface is driven both by their large polarizability and size

and by the neutralization of the surface plagued by the TBA cations. The relative importance of the latter effect increases with the enhanced positive charge density at the interface, i.e. with increasing concentration of the surfactant cations. The density profiles for  $\text{TBA}^+$  and  $\Gamma$  overlap with each other, while the  $\text{Br}^-$  interfacial peak is slightly shifted towards the bulk phase. For systems with bromide as the only counteranion we expect similar behavior as for iodide, i.e. mostly overlapping  $\text{TBA}^+$  and  $\text{Br}^-$  densities, however, with a lower surface peak of bromide compared to iodide (iodide affinity to the surface is higher due to its large polarizability and size). This would also explain the experimentally observed lower  $\text{Br}^-$  enrichment in the topmost layer for TBABr polar solutions when compared to  $\text{I}^-$  enrichment in TBAI solutions.<sup>26-28</sup> From our simulations of aqueous TBAF we learnt that fluoride, which is strongly repelled from the interface, tends to move by attractive Coulomb forces  $\text{TBA}^+$  toward the bulk phase, i.e. it effectively decreases surface concentration and, consequently, surface activity of the cationic surfactant. Analogically, since bromide is less surface active than iodide, a certain fraction of  $\text{TBA}^+$  in bromide solution tends to move toward the bulk phase, albeit the effect is much weaker than for fluoride as counter-anion. The experimentally observed lower surface activity of TBABr when compared to TBAI in polar solvents<sup>26-28</sup> can be then viewed as a consequence of the anionic specificity in the propensity for the air/solution interface.

#### **IV Conclusions**

Photoelectron spectroscopy and molecular dynamics simulations were employed to investigate the counter-anion specificity at the vacuum/solution interface of tetrabutyl-ammonium iodide in aqueous sodium bromide. The most important result, emerging from both experiment and calculations is that iodide is more enhanced in the interfacial layer, covered by surface-active tetrabutyl-ammonium cations, compared to bromide. The cations are surface-bound due to hydrophobic interactions of the butyl chains, while the anions exhibit a propensity for the vacuum/solution interface due to their appreciable polarizability and size, which are both larger for iodide than for bromide. This anion specificity also explains the experimentally observed lower activity of TBABr compared to TBAI in polar solvents.



## **Acknowledgement**

Support from the Czech Ministry of Education (grant No. LN00A032) and from the US-NSF (via the Environmental Molecular Science Institute) is gratefully acknowledged. Part of the work in Prague was completed within the framework of the Research Project Z4 055 905. We would like to thank the METAcenTer Project for providing computer facilities for our work.

## Figure captions

**Figure 1:** Photoelectron spectrum of 0.02 m TBAI, compared to that of 1m NaBr and a mixture of 1m NaBr and 0.02m TBAI aqueous solutions. Excitation energy was 100 eV.

**Figure 2:** Typical snapshots from MD simulations of a) a single TBAI ion pair, and b) 16 TBAI ion pairs in a slab containing 16 NaBr ion pairs and 863 water molecules. Color coding: TBA<sup>+</sup> - light blue and white, iodide – magenta, bromide – gold, sodium – green, water – red and white sticks.

**Figure 3:** Density profiles of a) dilute TBAI (single ion pair) and b) concentrated TBAI (16 ion pairs) in a 1 M NaBr solution across the aqueous slab.

Fig. 1:

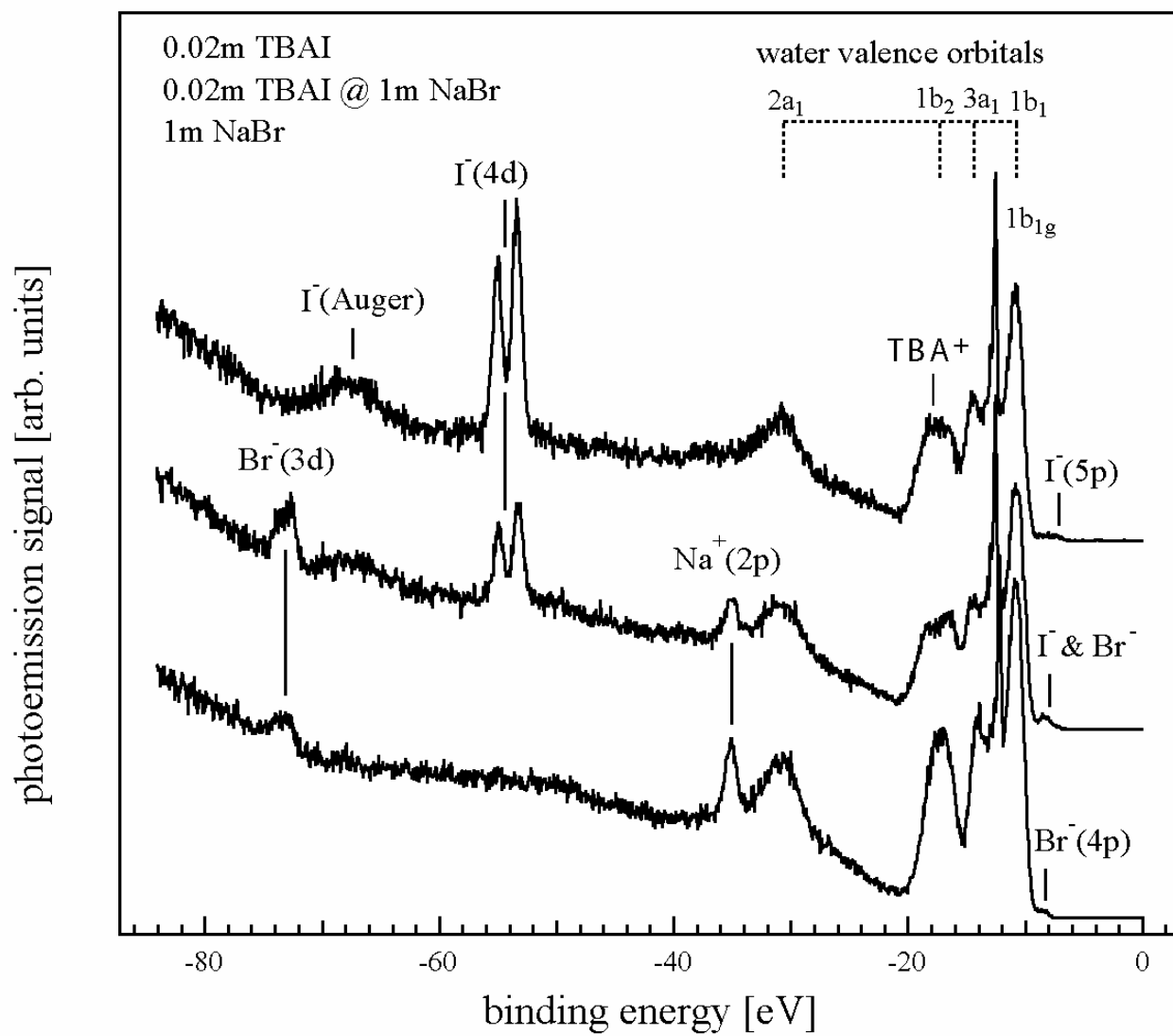


Fig. 2a:

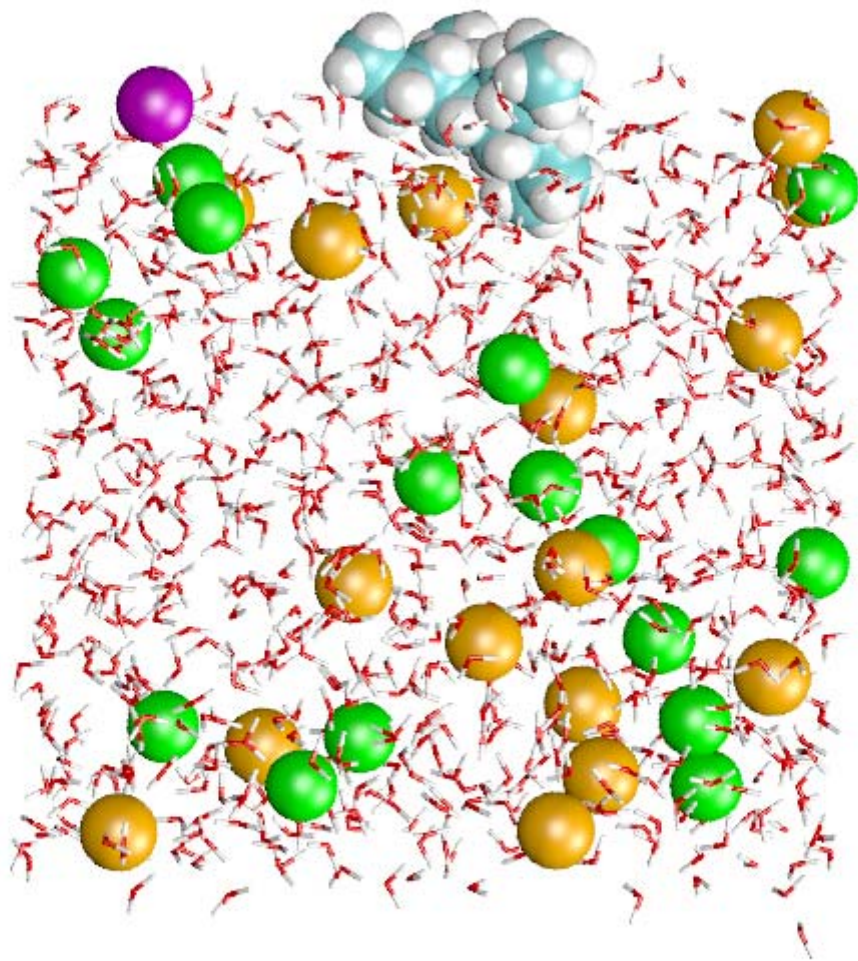


Fig. 2b:

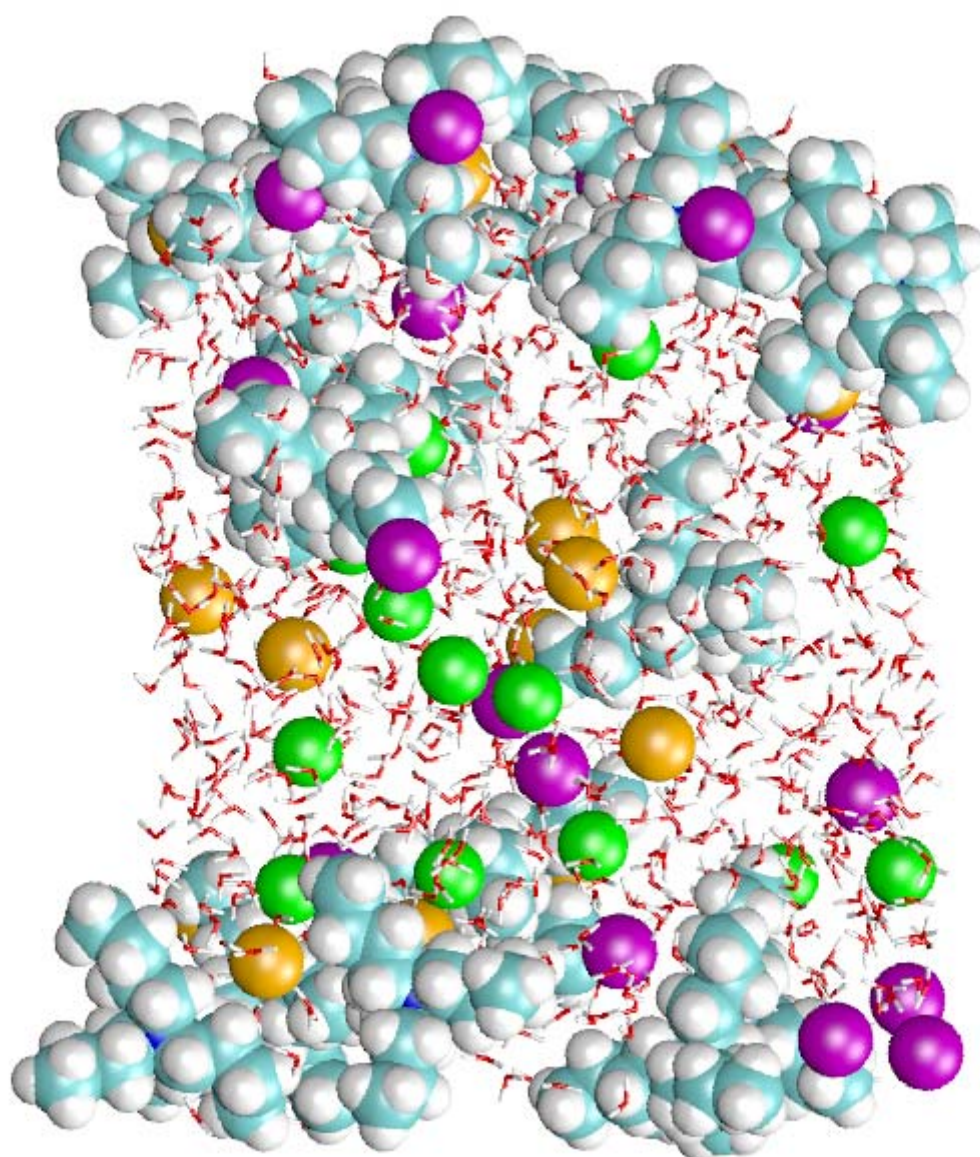


Fig. 3a:

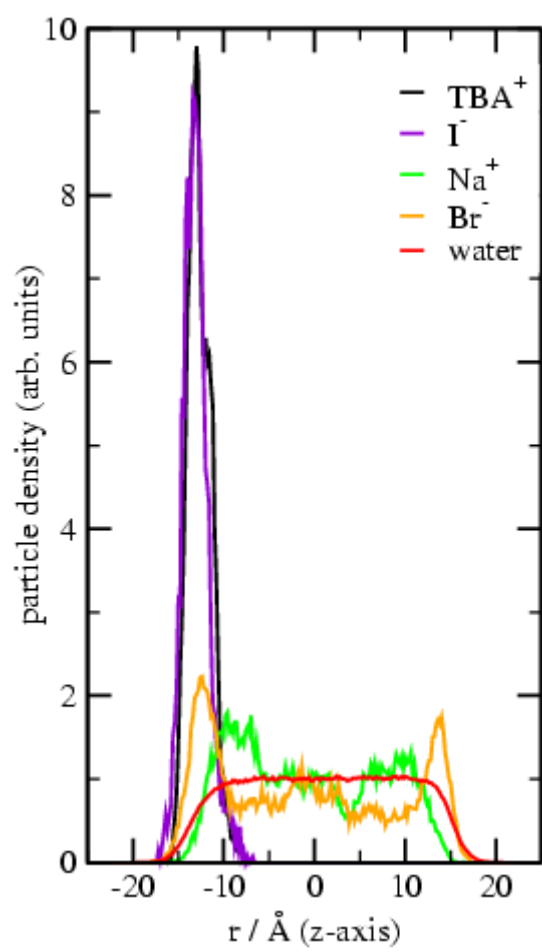
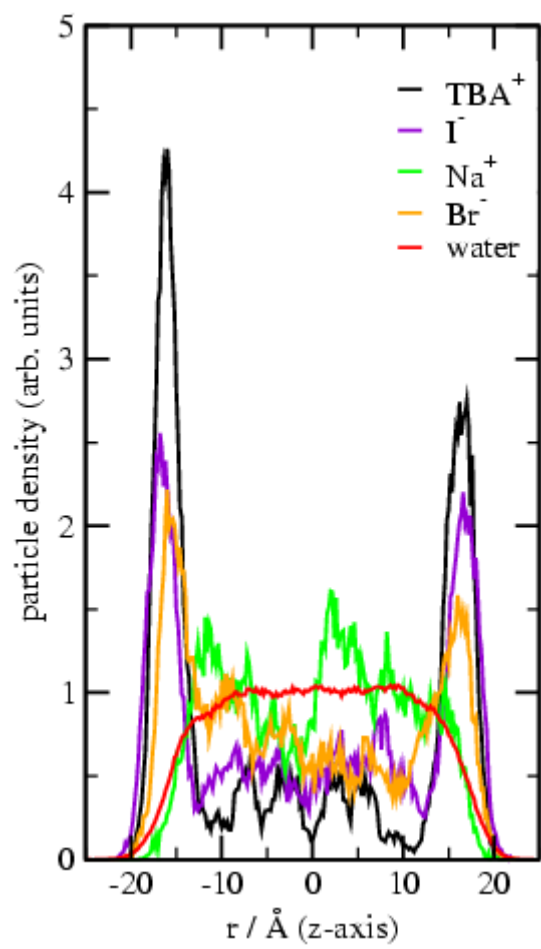


Fig. 3b:



## References

- (1) Liu, D. F.; Ma, G.; Levering, L. M.; Allen, H. C. *Journal of Physical Chemistry B* **2004**, *108*, 2252.
- (2) Petersen, P. B.; Johnson, J. C.; Knutsen, K. P.; Saykally, R. J. *Chemical Physics Letters* **2004**, *397*, 46.
- (3) Petersen, P. B.; Saykally, R. J. *Chemical Physics Letters* **2004**, *397*, 51.
- (4) Dang, L. X.; Chang, T. M. *Journal of Physical Chemistry B* **2002**, *106*, 235.
- (5) Jungwirth, P.; Tobias, D. J. *Journal of Physical Chemistry B* **2001**, *105*, 10468.
- (6) Vrbka, L.; Mucha, M.; Minofar, B.; Jungwirth, P.; Brown, E. C.; Tobias, D. J. *Current Opinion in Colloid & Interface Science* **2004**, *9*, 67.
- (7) Jungwirth, P.; Tobias, D. J. *Journal of Physical Chemistry B* **2002**, *106*, 6361.
- (8) Adam, N. K. *The Physics and Chemistry of Surfaces*; Oxford University Press: London, 1941.
- (9) Randalls, J. E. B. *Phys. Chem. Liq.* **1977**, *7*, 107.
- (10) Tarek, M.; Tobias, D. J.; Klein, M. L. *Journal of Physical Chemistry* **1995**, *99*, 1393.
- (11) Winter, B.; Weber, R.; Schmidt, P. M.; Hertel, I. V.; Faubel, M.; Vrbka, L.; Jungwirth, P. *Journal of Physical Chemistry B* **2004**, *108*, 14558.
- (12) Vrbka, L.; Jungwirth, P. *Australian Journal of Chemistry* **2004**, *57*, 1.
- (13) Moberg, R.; Bokman, F.; Bohman, O.; Siegbahn, H. O. G. *Journal of the American Chemical Society* **1991**, *113*, 3663.
- (14) Weber, R.; Winter, B.; Schmidt, P. M.; Widdra, W.; Hertel, I. V.; Dittmar, M.; Faubel, M. *Journal of Physical Chemistry B* **2004**, *108*, 4729.
- (15) Faubel, M.; Kisters, T. *Nature* **1989**, *339*, 527.
- (16) Winter, B.; Weber, R.; Widdra, W.; Dittmar, M.; Faubel, M.; Hertel, I. V. *Journal of Physical Chemistry A* **2004**, *108*, 2625.
- (17) Faubel, M.; Steiner, B.; Toennies, J. P. *Journal of Chemical Physics* **1997**, *106*, 9013.
- (18) Caldwell, J.; Dang, L. X.; Kollman, P. A. *Journal of the American Chemical Society* **1990**, *112*, 9144.
- (19) Essmann, U.; Perera, L.; Berkowitz, M. L.; Darden, T.; Lee, H.; Pedersen, L. G. *Journal of Chemical Physics* **1995**, *103*, 8577.



- (20) Ryckaert, J.-P.; Ciccotti, G.; Berendsen, H. J. C. *Journal of Computational Physics* **1977**, *23*, 327.
- (21) Case, D. A. P., D.A.; Caldwell, J.W.; Cheatham III, T.E.; Wang, J.; Ross, W.S.; Simmerling, C.L.; Darden, T.A.; Merz, K.M.; Stanton, R.V.; Cheng, A.L.; Vincent, J.J.; Crowley, M.; Tsui, V.; Gohlke, H.; Radmer, R.J.; Duan, Y.; Pitera, J.; Massova, I.; Seibel, G.L.; Singh, U.C.; Weiner, P.K.; Kollman, P.A. Amber7; Amber7, University of California: San Francisco, 2002.
- (22) Wang, J. M.; Cieplak, P.; Kollman, P. A. *Journal of Computational Chemistry* **2000**, *21*, 1049.
- (23) Perera, L.; Berkowitz, M. L. *Journal of Chemical Physics* **1994**, *100*, 3085.
- (24) Markovich, G.; Perera, L.; Berkowitz, M. L.; Cheshnovsky, O. *Journal of Chemical Physics* **1996**, *105*, 2675.
- (25) Hofmeister, F. *Arch. Exp. Pathol. Pharmacol. (Leipzig)* **1888**, *24*, 247.
- (26) Andersson, G.; Morgner, H. *Surface Science* **2000**, *445*, 89.
- (27) Eschen, F.; Heyerhoff, M.; Morgner, H.; Vogt, J. *Journal of Physics-Condensed Matter* **1995**, *7*, 1961.
- (28) Morgner, H.; Oberbrodthage, J.; Richter, K.; Roth, K. *Journal of Physics-Condensed Matter* **1991**, *3*, 5639.